Received: 26 June 2023 | Revised: 3 October 2023 | Accepted: 25 October 2023

DOI: 10.1002/jev2.12380

SHORT COMMUNICATION

Three-dimensional reconstruction of interstitial extracellular vesicles in human liver as determined by electron tomography

Roger Olofsson Bagge[1,2] | **Jens Berndtsson**[3] | **Ornella Urzì**[1,4] | **Jan Lötvall**[5] | **Massimo Micaroni**[3] | **Rossella Crescitelli**[1]

[1]Sahlgrenska Center for Cancer Research and Wallenberg Centre for Molecular and Translational Medicine, Department of Surgery, Institute of Clinical Sciences, Sahlgrenska Academy, University of Gothenburg, Gothenburg, Sweden

[2]Department of Surgery, Sahlgrenska University Hospital, Region Västra Götaland, Gothenburg, Sweden

[3]Centre for Cellular Imaging Core Facility, Sahlgrenska Academy, University of Gothenburg, Gothenburg, Sweden

[4]St. Anna Children's Cancer Research Institute (CCRI), Vienna, Austria

[5]Krefting Research Centre, Department of Internal Medicine and Clinical Nutrition, Institute of Medicine at Sahlgrenska Academy, University of Gothenburg, Gothenburg, Sweden

Correspondence
Rossella Crescitelli, Sahlgrenska Center for Cancer Research and Wallenberg Centre for Molecular and Translational Medicine, Department of Surgery, Institute of Clinical Sciences, Sahlgrenska Academy, University of Gothenburg, Gothenburg, Sweden.
Email: rossella.crescitelli@gu.se

Funding information
Wilhelm och Martina Lundgrens Vetenskapsfond, Grant/Award Number: 2023-SA-4142; Wallenberg Centre for Molecular and Translational Medicine; Knut och Alice Wallenbergs Stiftelse; Swedish Cancer Foundation; Assar Gabrielsson's foundation, Grant/Award Number: FB21-113; Vetenskapsrådet; Anna Lisa and Björnssons foundation

Abstract

Extracellular vesicles (EVs) are lipid bilayer nanoparticles involved in cell-cell communication that are released into the extracellular space by all cell types. The cargo of EVs includes proteins, lipids, nucleic acids, and metabolites reflecting their cell of origin. EVs have recently been isolated directly from solid tissues, and this may provide insights into how EVs mediate communication between cells in vivo. Even though EVs have been isolated from tissues, their point of origin when they are in the interstitial space has been uncertain. In this study, we performed three-dimensional (3D) reconstruction using transmission electron tomography of metastatic and normal liver tissues with a focus on the presence of EVs in the interstitium. After chemical fixation of the samples and subsequent embedding of tissue pieces in resin, ultrathin slices (300 nm) were cut and imaged on a 120 ekV transmission electron microscopy as a tilt series (a series of subsequent images tilted at different angles). These were then computationally illustrated in a 3D manner to reconstruct the imaged tissue volume. We identified the cells delimiting the interstitial space in both types of tissues, and small distinct spherical structures with a diameter of 30–200 nm were identified between the cells. These round structures appeared to be more abundant in metastatic tissue compared to normal tissue. We suggest that the observed spherical structures in the interstitium of the metastatic and non-metastatic liver represent EVs. This work thus provides the first 3D visualization of EVs in human tissue.

KEYWORDS
3D reconstruction, electron tomography, extracellular vesicles, melanoma tissue

1 | INTRODUCTION

To understand how extracellular vesicles (EVs) function in human health and disease, EVs need to be isolated from human sources. Most research has been performed on the EV secretome from human cells cultured in vitro, and some of the mechanistic functions of EVs have been described in that way (Yanez-Mo et al., 2015). However, isolating EVs from healthy or diseased

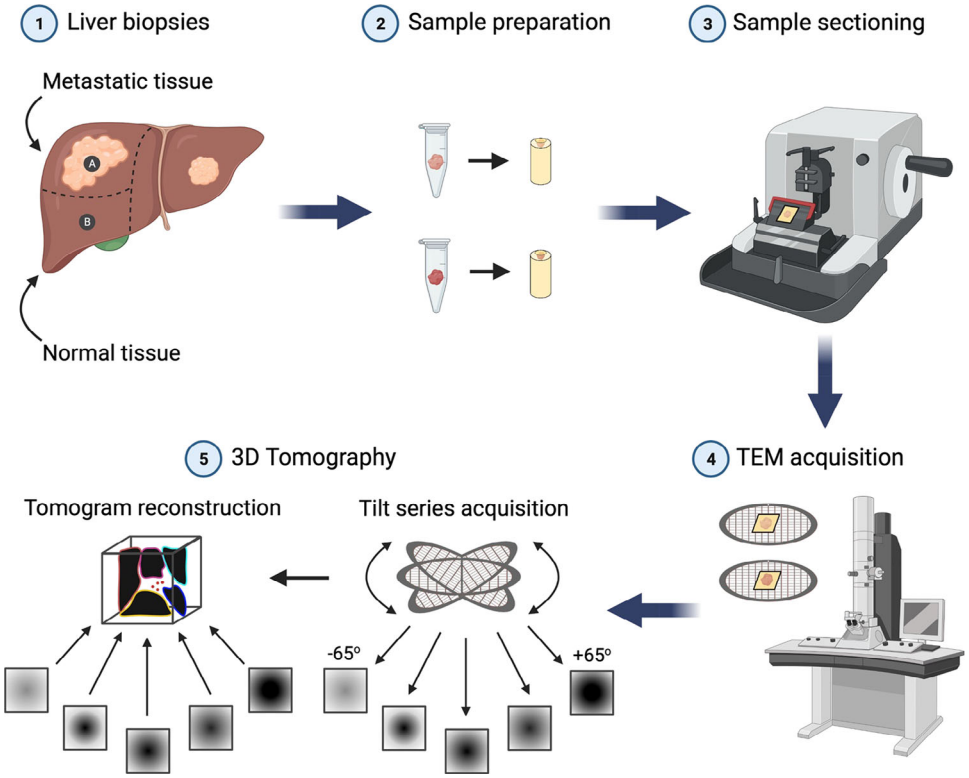

FIGURE 1 Schematic illustration of the steps involved in the acquisition of the 3D reconstructions by electron tomography of tissues. Metastatic liver tissue and macroscopically normal liver tissue were collected from the liver of a patient with uveal melanoma liver metastases. Samples were fixed, dehydrated, and embedded in resin. Sections of 300 nm thickness were obtained using a microtome. During the electron tomography data acquisition, the specimen holder was gradually tilted inside the microscope around an axis perpendicular to the electron beam, and subsequent frames were then acquired at multiple angles (+65° and −65°). Finally, a 3D reconstruction (tomogram) of the tissue was computed from the acquired images using the IMOD program. Figure created using BioRender.com.

tissues has until now primarily utilized biological fluids such as blood, saliva, urine, ejaculates, breast milk, and cerebrospinal fluid (Admyre et al., 2007; Baranyai et al., 2015), and although these experiments have identified many biomarker candidates for various diseases, they have not provided much information on EV function. To learn how EVs mediate communication between cells, we need to begin studying how they are trafficked in intact tissues. However, efforts to isolate EVs from tissues have only recently been initiated (Crescitelli et al., 2020, 2021; Hurwitz et al., 2019; Jang et al., 2019; Vella et al., 2017), and there is still some uncertainty as to whether the isolated tissue-derived vesicles are indeed extracellular and not contaminations from the intracellular compartments of tissue cells.

We therefore hypothesized that EVs can be illustrated in tissues using transmission electron tomography. To do this, we acquired human liver biopsies that were chemically fixed and embedded in resin. We cut 300 nm sections from both apparently non-tumour liver sections and liver sections with obvious uveal melanoma metastasis. Several images of the same area were acquired while the section was tilted in the transmission electron microscope (TEM). Image analysis software was then used to create a three-dimensional (3D) illustration of the tissue, including the interstitial space.

2 | METHODS

The methods utilized for preparing the tissues and for the imaging are presented in Supporting information.

2.1 | Workflow

We collected liver metastatic tissue and macroscopically normal-appearing liver tissue samples from a patient with stage IV uveal melanoma. The samples were fixed using chemical fixation, dehydrated, and embedded in resin. The samples were then sectioned with a thickness of 300 nm, and tilted images were acquired on the TEM from different angles (frames), which were then computationally back projected into a 3D space along the same angles to recreate a 3D volume of the imaged sample (Figure 1).

3 | RESULTS

Liver metastatic tissue and macroscopically normal liver tissue were processed as described in Figure 1 to obtain a 3D reconstruction of the tissue interstitial space. In each acquired image we focused on cells and round elements present in the extracellular space. In the tumour tissue sections, three cells with surrounding extended extracellular space containing several spherical elements of different sizes were identified (Figure 2a). Specifically, six large distinct structures (1–2 μm—not confluent with cells) were clearly visible in the intercellular space accompanied by smaller round elements (<200 nm). We hypothesize that the larger structures are morphologically similar to apoptotic bodies and that the smaller structures are morphologically similar to small EVs. To facilitate the visualization, the previously described structures were labelled with colours by the imaging software, in which the three cells were highlighted in yellow, turquoise, and green, respectively (Figure 2b). The larger structures present in the extracellular space were labelled blue, and the smaller round elements were labelled red. Three different frames from Video 1 show the front, −30°, and +30° sides of the tissue section (Figure 2c–e). The 3D reconstruction of the sample was obtained by merging all of the acquired frames from the tomography process, thus allowing better visualization of the entire tissue section (Video 1). The 3D tomography reconstruction clearly illustrated that the small round structures located in the extracellular space had spherical morphology and a size comparable to canonical EVs (50–200 nm) (Thery et al., 2018). Moreover, as shown in Supplementary Video 1, it is possible to visualize the single images in the sequence used for the 3D reconstruction. In the first part of the video, small round structures in the extracellular space, which could be small EVs, are indicated by white arrows, while in the second part cell membranes are highlighted in green, yellow, and turquoise, the large round structures (apoptotic bodies) are highlighted in blue, and the small round structures (small EVs) are highlighted in red.

We performed the same analysis on the macroscopically normal liver tissue collected from the same patient. Figure 3(a) shows a representative image of the tilt series, where five cells were clearly visible with their intracellular organelles and their plasma membranes, which delimited the extracellular space. The presence of small round structures was less evident compared to the tumour tissue because of their smaller size and internal position within the section. The above-mentioned structures are underlined with different colours in Figure 3(b) where five cells are labelled with green, yellow, turquoise, orange, and magenta and the small round structures (small EVs) are highlighted in red. The 3D reconstruction of the sample was obtained by merging all of the acquired frames during the tomography process, thus allowing a better visualization of the entire tissue section (Video 2). Three different frames of Video 2 showing the front, −30°, and +30° sides of normal tissue sections are presented in Figure 3(c–e), respectively. In the 3D reconstruction of normal tissue shown in Supplementary Video 2, single images in the sequence used for the 3D reconstruction are shown. Moreover, the small round elements present in the extracellular space were more apparent than in the 2D picture (Figure 3a). Although apparently less abundant than in metastatic tissue, the spherical shape of these round elements is clear, again suggesting that they are small EVs (30–150 nm). The small round structures are highlighted with white arrows in the first part of the video. In the second part of the video, the cells are highlighted in green, yellow, turquoise, orange, and magenta, while the small structures (putative small EVs) are marked in red (Supplementary Video 2).

4 | DISCUSSION

In this work we have visualized round structures in the interstitial space of human liver tissues using electron tomography, and we suggest that these are most likely EVs released by local cells. The tomography was performed on both liver metastases and normal liver tissue samples from a single patient affected by uveal melanoma. In both types of samples, we identified small round EV structures in the extracellular space but could also illustrate the presence of apparent cell protrusions extending from cells that if cut horizontally using 2D techniques could appear as round elements and wrongly be described as EVs.

EVs are usually visualized after isolation and not in their native environment. The isolation process and sample preparation may lead to the creation of artefacts, altering the native EV structure. A proof of this is the canonical 'cup shape' morphology of EVs observed using TEM that is an artefact caused by the high surface tension of water (Kurtjak et al., 2022; Rikkert et al., 2019). Moreover, depending on the biological origin of the sample (cell culture media, biological fluids, or tissues) EVs are co-isolated with other biological structures that co-precipitate thus decreasing EV sample purity and confounding the analyses of electron microscopy imaging. Another approach to visualizing EVs in their natural environment is thin sectioning of the tissue after fixation, dehydration, and embedding in plastic (Crescitelli et al., 2020, 2021). However, the thin sectioning process provides a 2D image that cannot visualize the end of each structure, and a round membrane structure could potentially be wrongly attributed as an EV even though it may be a cell membrane protrusion still connected to a cell. The 3D reconstruction of interstitial tissues may help to overcome this limitation and allow for better visualization of EVs within different types of tissues.

Even though these specific electron tomographs seemed to visualize higher numbers of interstitial EVs in the tumour tissues than in the apparent healthy tissue, it is impossible to conclude that there are true numeric differences between tumour tissues and healthy liver tissues. This question is of course interesting but would require a very large number of tomographs from multiple patients, which would be exceptionally resource consuming. Even though this study shows that EVs can be illustrated in the

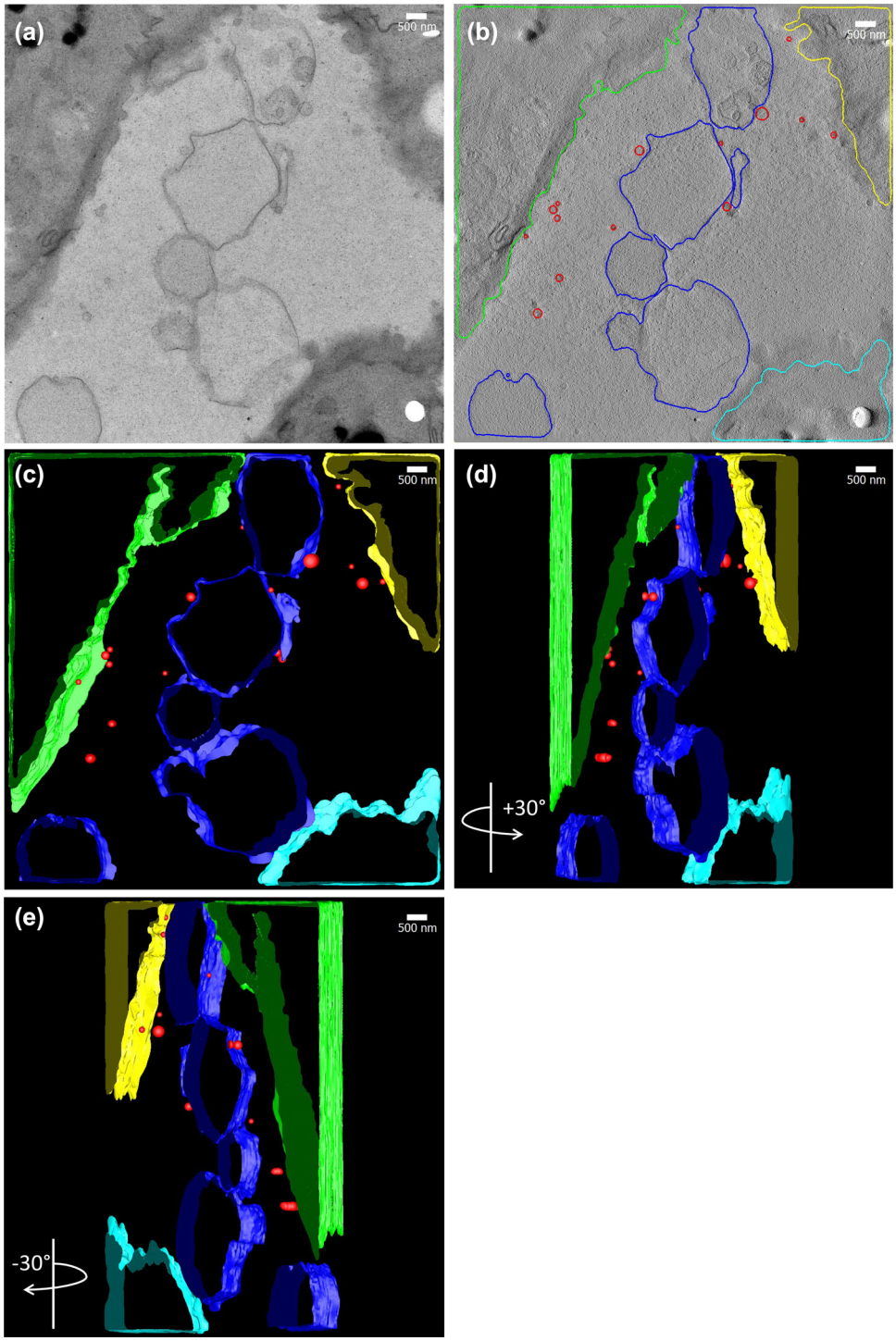

FIGURE 2 The 3D reconstruction of melanoma metastatic tissue. (a) Transmission electron microscopy image showing three cells and large structures as well as small spherical structures in between the cells. (b) The cells are visualized by computer-added colours (green, yellow, and turquoise), and the large structures in the extracellular space are indicated in darker blue, whereas the smaller spherical structures are indicated in red. (c-d-e) 3D model shown frontally (c) and rotated at (d) +30° and (e) −30° along the y-axis.

interstitial space, we are not suggesting that researchers studying tissue-derived EVs would have to provide such data. It is possible that future technology development, such as rapid high-throughput electron tomography, will make it easier to perform such studies.

The technology described here opens to new opportunities to further investigate the fate of EV distribution in tissues. The technique may allow for the identification of specific EV surface marker, using either fluorescence- or gold- labelled antibodies

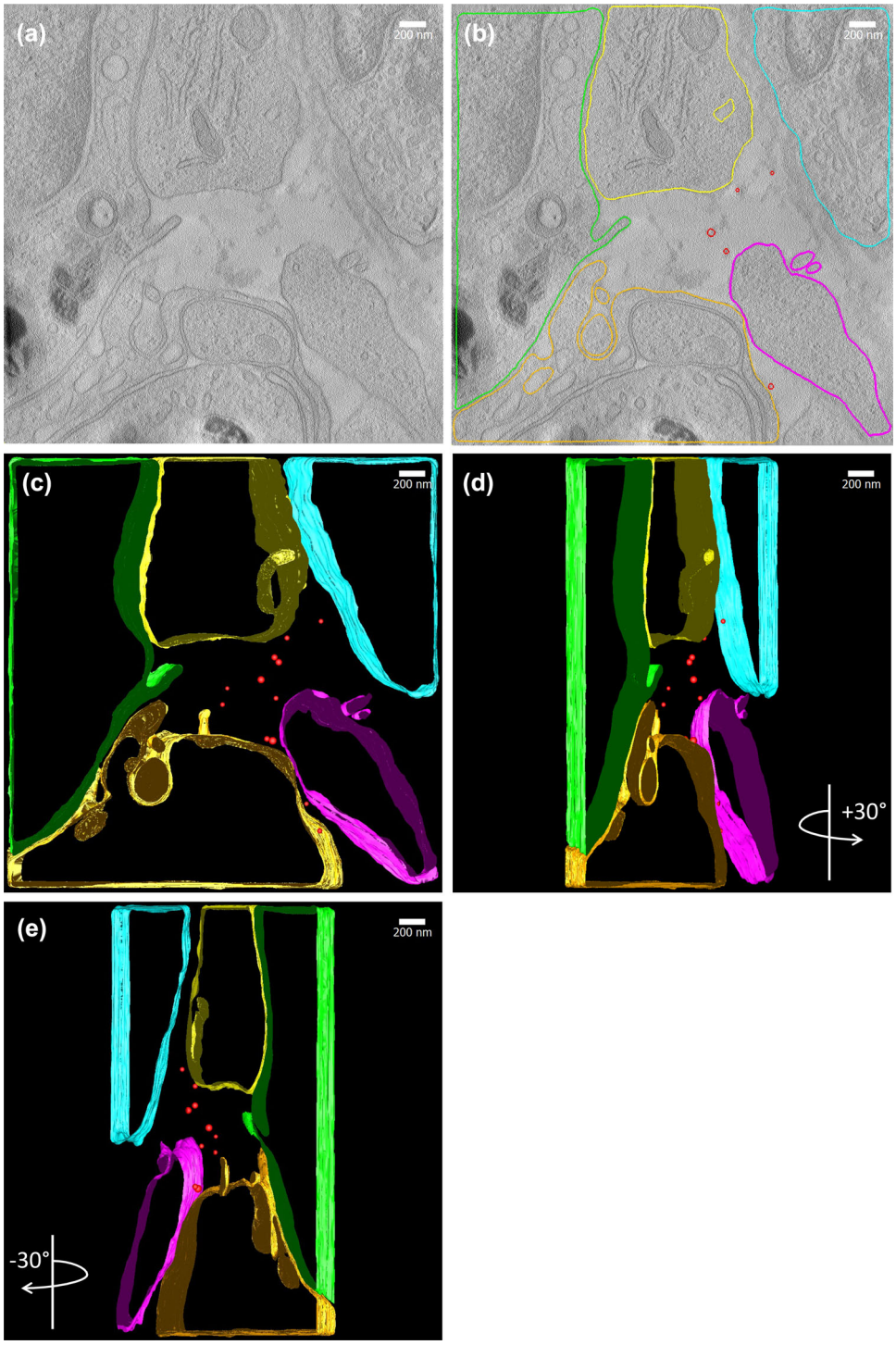

FIGURE 3 The 3D reconstruction of non-tumour tissue. (a) Transmission electron microscopy image showing three cells and large structures as well as small spherical structures in between the cells. (b) The cells are visualized by computer-added colours (green, yellow, turquoise, magenta, and orange), and the smaller spherical structures are indicated in red. (c-d-e) 3D model shown frontally (c) and rotated at (d) +30° and (e) −30° along the y-axis.

that may visualize specific EVs subtypes in the 3D TEM tomography. In this way, it may even be possible to identify the in vivo tissue distribution of EVs at the nanometre level, shedding light on which cells take up the EVs, as well as on the EV intracellular fate.

Six larger non-cellular structures (highlighted in blue) were observed in the tumour-tissue derived tomographs. These may either be apoptotic bodies, necrotic vesicles, or large oncosomes. Apoptotic bodies are produced during programmed cell death in both healthy and tumour tissues and are very large EVs (50−5000 nm) that are size-wise similar to those illustrated in these

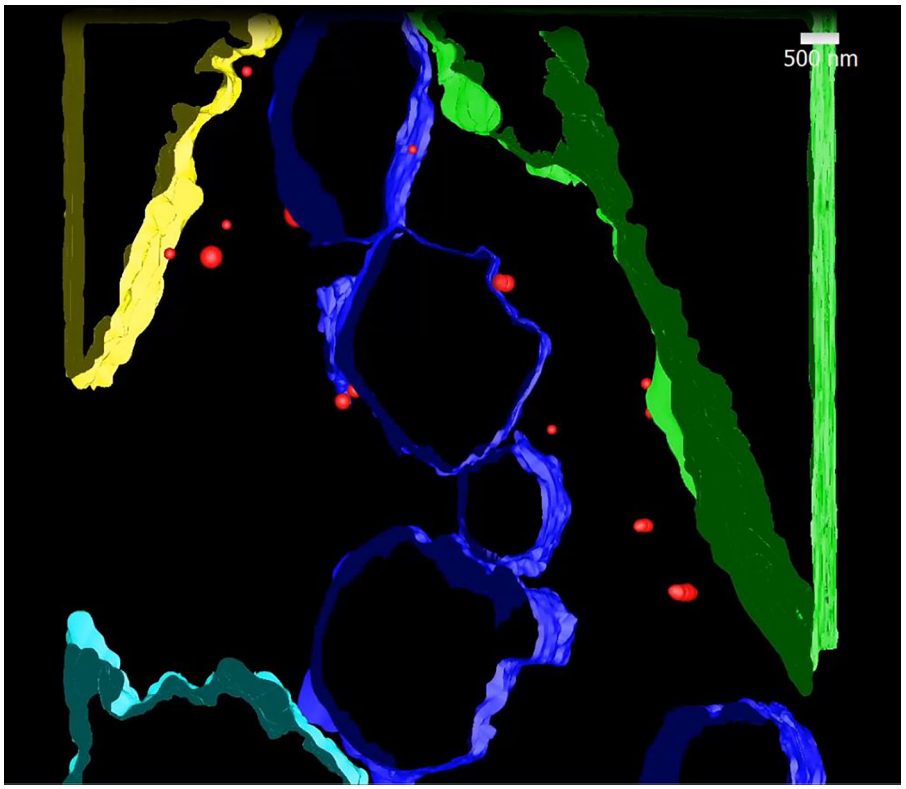

Video 1 Electron tomography reconstruction of melanoma metastatic tissue. In the first part of the video, the 3D reconstruction of melanoma metastatic tissue is shown from all angles rotating the model around the y-axis. In the second part the same tissue is shown with a focus on a group of small EVs (in red) shown from all angles with the same rotation. The full-text HTML version of this article includes video content. To view this version please visit https://onlinelibrary.wiley.com/doi/10.1002/jev2.12380.

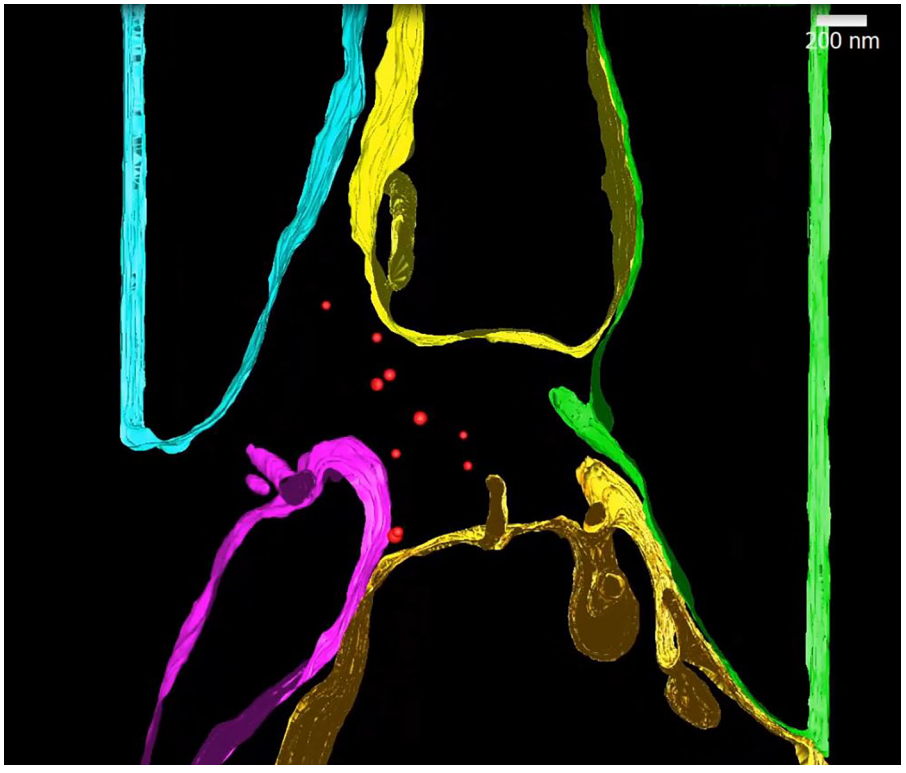

Video 2 Electron tomography reconstruction of non-tumour tissue. In the first part of the video, the 3D reconstruction of non-tumour tissue is shown from all angles rotating the model around the y-axis. In the second part the same tissue is shown with a focus on a group of small EVs (in red) shown from all angles with the same rotation described above. The full-text HTML version of this article includes video content. To view this version please visit https://onlinelibrary.wiley.com/doi/10.1002/jev2.12380.

tomograms (Kakarla et al., 2020). These larger structures were not seen in the tomograms of apparently healthy tissues but may very well be found if larger numbers of biopsies are studied.

The 3D reconstruction of both tumour and normal tissues showed that the small round structures, which are believed to be EVs, are spherical. This is in concordance with previous studies demonstrating that the round shape of EVs is given by their protein and lipid composition, which causes the membrane curvature (Huang et al., 2017; Kastelowitz & Yin, 2014). However, a round shape is not the only phenotype described for EVs. Arraud et al. isolated and characterized EVs from blood plasma and showed that platelet-free plasma contains both spherical and tubular EVs (Arraud et al., 2014). The origin of those tubular EVs may be the direct fragmentation of vascular cells (Arraud et al., 2014); moreover, as mentioned above, the microenvironment can have an impact on EV morphology (Logozzi et al., 2018; Shao et al., 2018). This could be the reason why blood EVs possess both spherical and tubular shapes, while in tissues we observed predominantly round morphology.

In this study, samples were fixed using a chemical fixation protocol, which is the most commonly used technique to preserve cell and tissue structures in the biological sciences (Graham & Orenstein, 2007), but we cannot exclude the possibility that vesicles are released from cells during that process (Li et al., 2017; Collett et al., 2018). Nevertheless, chemical fixation still represents a valuable and broadly used protocol for electron microscopy imaging (Graham & Orenstein, 2007). Moreover, to limit possible biases we processed both tumour and non-tumour liver tissues, which could be considered to be our internal control sample.

5 | CONCLUSION

In summary, we have provided a 3D visualization of apparent EVs in their tissue microenvironment, both in metastatic and normal liver tissues, thus demonstrating for the first time the presence and spherical shape of EVs in the interstitial space of tissues.

AUTHOR COTRIBUTIONS

Roger Olofsson Bagge: Conceptualization; funding acquisition; supervision; writing—review and editing. **Jens Berndtsson**: Data curation; methodology; writing—review and editing. **Ornella Urzì**: Writing—original draft. **Jan Lötvall**: Conceptualization; writing—review and editing. **Massimo Micaroni**: Formal analysis; methodology; writing—review and editing. **Rossella Crescitelli**: Conceptualization; data curation; funding acquisition; investigation; methodology; resources; supervision; writing—original draft; writing—review and editing.

ACKNOWLEDGEMENTS

We acknowledge the Centre for Cellular Imaging (CCI) at University of Gothenburg and the National Microscopy Infrastructure, NMI (VR-RFI 2019-00217) for providing assistance in microscopy. Major funding was received from the Swedish Cancer Foundation, the Swedish Research Council, the Knut and Alice Wallenberg Foundation, and the Wallenberg Centre for Molecular and Translational Medicine, University of Gothenburg, Sweden. Rossella Crescitelli was supported by the Assar Gabrielsson's foundation (Grant # FB21-113), the Anna Lisa and Björnssons foundation, the Wilhelm och Martina Lundgrens Vetenskapsfond (2023-SA-4142), the Knut and Alice Wallenberg Foundation, and the Wallenberg Centre for Molecular and Translational Medicine, University of Gothenburg, Sweden.

CONFLICT OF INTEREST STATEMENT

Rossella Crescitelli and Jan Lötvall have developed multiple EV-associated patents for putative clinical utilization. Rossella Crescitelli owns equity in Exocure Sweden AB. Jan Lötvall owns equity in Exocure Sweden AB and Nexocure Therapeutics AB and consults in the field of EVs through Vesiclebio AB. Roger Olofsson Bagge has received institutional research grants from Bristol-Myers Squibb, Endomagnetics Ltd. (Endomag), and SkyLineDx; has received speaker honoraria from Roche, Pfizer, and Pierre-Fabre; has served on advisory boards for Amgen, BD/BARD, Bristol-Myers Squibb, Merck Sharp & Dohme, Novartis, Roche, and Sanofi Genzyme; and is a shareholder in SATMEG Ventures AB.

ORCID

Jens Berndtsson https://orcid.org/0000-0001-6627-8134
Rossella Crescitelli https://orcid.org/0000-0002-1714-3169

REFERENCES

Admyre, C., Johansson, S. M., Qazi, K. R., Filén, J.-J., Lahesmaa, R., Norman, M., Neve, E. P. A., Scheynius, A., & Gabrielsson, S. (2007). Exosomes with immune modulatory features are present in human breast milk. *Journal of Immunology*, *179*, 1969–1978.

Arraud, N., Linares, R., Tan, S., Gounou, C., Pasquet, J.-M., Mornet, S., & Brisson, A. R. (2014). Extracellular vesicles from blood plasma: Determination of their morphology, size, phenotype and concentration. *Journal of Thrombosis and Haemostasis*, *12*, 614–627.

Baranyai, T., Herczeg, K., Onódi, Z., Voszka, I., Módos, K., Marton, N., Nagy, G., Mäger, I., Wood, M. J., El Andaloussi, S., Pálinkás, Z., Kumar, V., Nagy, P., Kittel, Á., Buzás, E. I., Ferdinandy, P., & Giricz, Z. (2015). Isolation of exosomes from blood plasma: qualitative and quantitative comparison of ultracentrifugation and size exclusion chromatography methods. *PLoS ONE*, *10*, e0145686.

Collett, G. P., Redman, C. W., Sargent, I. L., & Vatish, M. (2018). Endoplasmic reticulum stress stimulates the release of extracellular vesicles carrying danger-associated molecular pattern (DAMP) molecules. *Oncotarget*, *9*, 6707–6717.

Crescitelli, R., Lässer, C., Jang, S. C., Cvjetkovic, A., Malmhäll, C., Karimi, N., Höög, J. L., Johansson, I., Fuchs, J., Thorsell, A., Gho, Y. S., Olofsson Bagge, R., & Lötvall, J. (2020). Subpopulations of extracellular vesicles from human metastatic melanoma tissue identified by quantitative proteomics after optimized isolation. *Journal of Extracellular Vesicles*, *9*, 1722433.

Crescitelli, R., LäSser, C., & LöTvall, J. (2021). Isolation and characterization of extracellular vesicle subpopulations from tissues. *Nature Protocols*, *16*, 1548–1580.

Graham, L., & Orenstein, J. M. (2007). Processing tissue and cells for transmission electron microscopy in diagnostic pathology and research. *Nature Protocols*, *2*, 2439–2450.

Huang, C., Quinn, D., Sadovsky, Y., Suresh, S., & Hsia, K. J. (2017). Formation and size distribution of self-assembled vesicles. *PNAS*, *114*, 2910–2915.

Hurwitz, S. N., Olcese, J. M., & Meckes, D. G., jr. (2019). Extraction of extracellular vesicles from whole tissue. *Journal of Visualized Experiments: JoVE*, *144*, https://doi.org/10.3791/59143

Jang, S. C., Crescitelli, R., Cvjetkovic, A., Belgrano, V., Bagge, R. O., Sundfeldt, K., Ochiya, T., Kalluri, R., & Lötvall, J. (2019). Mitochondrial protein enriched extracellular vesicles discovered in human melanoma tissues can be detected in patient plasma. *Journal of Extracellular Vesicles*, *8*, 1635420.

Kakarla, R., Hur, J., Kim, Y. J., Kim, J., & Chwae, Y.-J. (2020). Apoptotic cell-derived exosomes: Messages from dying cells. *Experimental & Molecular Medicine*, *52*, 1–6.

Kastelowitz, N., & Yin, H. (2014). Exosomes and microvesicles: Identification and targeting by particle size and lipid chemical probes. *Chembiochem*, *15*, 923–928.

Kremer, J. R., Mastronarde, D. N., & Mcintosh, J. R. (1996). Computer visualization of three-dimensional image data using IMOD. *Journal of Structural Biology*, *116*, 71–76.

Kurtjak, M., Kereïche, S., Klepac, D., Križan, H., Perčić, M., Krušić Alić, V., Lavrin, T., Lenassi, M., Wechtersbach, K., Kojc, N., Vukomanović, M., Zrna, S., Biberić, M., Domitrović, R., Grabušić, K., & Malenica, M. (2022). Unveiling the native morphology of extracellular vesicles from human cerebrospinal fluid by atomic force and cryogenic electron microscopy. *Biomedicines*, *10*, 1251.

Li, Y., Almassalha, L. M., Chandler, J. E., Zhou, X., Stypula-Cyrus, Y. E., Hujsak, K. A., Roth, E. W., Bleher, R., Subramanian, H., Szleifer, I., Dravid, V. P., & Backman, V. (2017). The effects of chemical fixation on the cellular nanostructure. *Experimental Cell Research*, *358*, 253–259.

Logozzi, M., Mizzoni, D., Angelini, D., Di Raimo, R., Falchi, M., Battistini, L., & Fais, S. (2018). Microenvironmental pH and exosome levels interplay in human cancer cell lines of different histotypes. *Cancers (Basel)*, *10*, 370.

Mastronarde, D. N. (1997). Dual-axis tomography: An approach with alignment methods that preserve resolution. *Journal of Structural Biology*, *120*, 343–352.

Rikkert, L. G., Nieuwland, R., Terstappen, L. W. M. M., & Coumans, F. A. W. (2019). Quality of extracellular vesicle images by transmission electron microscopy is operator and protocol dependent. *Journal of Extracellular Vesicles*, *8*, 1555419.

Shao, C., Yang, F., Miao, S., Liu, W., Wang, C., Shu, Y., & Shen, H. (2018). Role of hypoxia-induced exosomes in tumor biology. *Molecular Cancer*, *17*, 120.

Théry, C., Witwer, K. W., Aikawa, E., Alcaraz, M. J., Anderson, J. D., Andriantsitohaina, R., Antoniou, A., Arab, T., Archer, F., Atkin-Smith, G. K., Ayre, D. C., Bach, J.-M., Bachurski, D., Baharvand, H., Balaj, L., Baldacchino, S., Bauer, N. N., Baxter, A. A., Bebawy, M., & Zuba-Surma, E. K. (2018). Minimal information for studies of extracellular vesicles 2018 (MISEV2018): A position statement of the International Society for Extracellular Vesicles and update of the MISEV2014 guidelines. *Journal of Extracellular Vesicles*, *7*, 1535750.

Vella, L. J., Scicluna, B. J., Cheng, L., Bawden, E. G., Masters, C. L., Ang, C.-S., Willamson, N., Mclean, C., Barnham, K. J., & Hill, A. F. (2017). A rigorous method to enrich for exosomes from brain tissue. *Journal of Extracellular Vesicles*, *6*, 1348885.

Yáñez-Mó, M., Siljander, P. R.-M., Andreu, Z., Bedina Zavec, A., Borràs, F. E., Buzas, E. I., Buzas, K., Casal, E., Cappello, F., Carvalho, J., Colás, E., Cordeiro-Da Silva, A., Fais, S., Falcon-Perez, J. M., Ghobrial, I. M., Giebel, B., Gimona, M., Graner, M., Gursel, I., & De Wever, O. (2015). Biological properties of extracellular vesicles and their physiological functions. *Journal of Extracellular Vesicles*, *4*, 27066.

SUPPORTING INFORMATION

Additional supporting information can be found online in the Supporting Information section at the end of this article.

How to cite this article: Olofsson Bagge, R., Berndtsson, J., Urzì, O., Lötvall, J., Micaroni, M., & Crescitelli, R. (2023). Three-Dimensional reconstruction of interstitial extracellular vesicles in human liver as determined by electron tomography. *Journal of Extracellular Vesicles*, *12,* e12380. https://doi.org/10.1002/jev2.12380